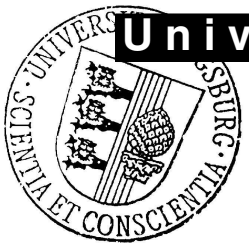

Universität Augsburg

Institut für
Mathematik

Ronald H.W. Hoppe, Irwin Yousept

Adaptive Edge Element Approximation of H(curl)-Elliptic Optimal Control Problems with Control Constraints

Preprint Nr. 19/2013 — 11. Oktober 2013
Institut für Mathematik, Universitätsstraße, D-86135 Augsburg http://www.math.uni-augsburg.de/

Impressum:

Herausgeber:

Institut für Mathematik
Universität Augsburg
86135 Augsburg
`http://www.math.uni-augsburg.de/de/forschung/preprints.html`

ViSdP:

Ronald H.W. Hoppe
Institut für Mathematik
Universität Augsburg
86135 Augsburg

ADAPTIVE EDGE ELEMENT APPROXIMATION OF H(CURL)-ELLIPTIC OPTIMAL CONTROL PROBLEMS WITH CONTROL CONSTRAINTS

RONALD H. W. HOPPE* AND IRWIN YOUSEPT†

Abstract. A three-dimensional **H**(**curl**)-elliptic optimal control problem with distributed control and pointwise constraints on the control is considered. We present a residual-type a posteriori error analysis with respect to a curl-conforming edge element approximation of the optimal control problem. Here, the lowest order edge elements of Nédélec's first family are used for the discretization of the state and the control with respect to an adaptively generated family of simplicial triangulations of the computational domain. In particular, the a posteriori error estimator consists of element and face residuals associated with the state equation and the adjoint state equation. The main results are the reliability of the estimator and its efficiency up to oscillations in terms of the data of the problem. In the last part of the paper, numerical results are included which illustrate the performance of the adaptive approach.

Key words. Optimal control of PDEs, H(curl)-elliptic problems, curl-conforming edge elements, residual a posteriori error estimator, reliability and efficiency.

AMS subject classifications. Primary: 65K10; Secondary: 49M05,65N30,65N50,78M10

1. Introduction. This paper is devoted to an a posteriori error analysis of adaptive edge element methods for control constrained distributed optimal control of **H**(**curl**)-elliptic problems in $\mathbb{R}^3$. Adaptive edge element methods for **H**(**curl**)-elliptic boundary value problems on the basis of residual-type a posteriori error estimators have been initiated in [7, 8, 31] and later on considered in [11, 35]. A convergence analysis has been provided in [24]. For nonstandard discretizations such as Discontinuous Galerkin methods, we refer to [12, 25]. In case of the time-harmonic Maxwell equations, convergence and quasi-optimality of adaptive edge element approximations have been established in [42, 46] in the spirit of the results obtained in [13] for linear second order elliptic boundary value problems.

We refer to [26, 39, 43, 44, 45] for recent results on the mathematical and numerical analysis of the optimal control of **H**(**curl**)-elliptic PDEs. To the best of our knowledge, this paper is the first contribution towards a residual-type a posteriori error analysis for **H**(**curl**)-elliptic optimal control problems. We are not aware of any previous studies in this direction. On the other hand, both residual-type a posteriori error estimators and dual weighted residuals for P1 conforming finite element approximations of control constrained $H^1(\Omega)$-elliptic optimal control problems have been developed in [17, 19, 27, 29] and [18, 41].

Adaptive Finite Element Methods (AFEMs) typically consist of successive loops of the sequence

$$\text{SOLVE} \rightarrow \text{ESTIMATE} \rightarrow \text{MARK} \rightarrow \text{REFINE} \,. \tag{1.1}$$

*Department of Mathematics, University of Houston, Houston, TX 77204-3008, USA (rohop@math.uh.edu), and Institute of Mathematics, University of Augsburg, D-86159 Augsburg, Germany (hoppe@math.uni-augsburg.de). The author acknowledges support by the NSF grants DMS-1115658, DMS-1216857, by the German National Science Foundation within the Priority Programs SPP 1253, SPP 1506, by the German Federal Ministry for Education and Research (BMBF) within the projects BMBF-FROPT and BMBF-MeFreSim, and by the European Science Foundation (ESF) within the ESF Program OPTPDE.

†Graduate School of Excellence Computational Engineering, Technical University Darmstadt, D-64293 Darmstadt, Germany (yousept@gsc.tu-darmstadt.de).

The first step SOLVE stands for the efficient solution of the finite element discretized problem with respect to a given triangulation of the computational domain. Efficient iterative solvers include multilevel techniques and/or domain decomposition methods. As far as their application to edge element discretizations of $\mathbf{H}(\mathbf{curl})$-elliptic problems is concerned, we refer to [3, 21] (cf. also the survey articles [4, 22] and the references therein). The second step ESTIMATE requires the a posteriori estimation of the global discretization error or some other error functional as a basis for an adaptive mesh refinement and will be in the focus of our paper. The following step MARK is devoted to the specification of elements of the triangulation that have to be selected for refinement in order to achieve a reduction of the error. Within the convergence analysis of AFEMs [9, 13, 15, 36] a so-called bulk criterion, meanwhile also known as Dörfler marking, has been investigated which will be adopted here. Finally, the last step REFINE realizes the refinement of the mesh. Here, we will use the newest vertex bisection.

This paper is organized as follows: The optimal control problem will be stated in section 2 with the optimality conditions being given in subsection 2.1 in terms of the state, the adjoint state, the control, and the Lagrangian multiplier. The control problem is discretized with respect to a shape regular family of simplicial triangulations of the computational domain using curl-conforming edge elements of Nédélec's first family for all relevant variables (see Section 2.2). The a posteriori error analysis involves a residual-type error estimator consisting of element and face residuals and oscillations associated with the data of the problem which will be introduced in subsection 2.3. The marking of elements for refinement by Dörfler marking and the adaptive refinement by newest vertex bisection will be briefy described in subsection 2.4. The main results, namely the reliability of the residual a posteriori error estimator and its efficiency up to data oscillations, will be established in section 3 and section 4. Finally, section 5 contains a documentation of numerical results illustrating the performance of the adaptive approach.

2. The optimal control problem and its edge element approximation.

2.1. The optimal control problem. We adopt standard notation from Lebesgue and Sobolev space theory (cf., e.g., [37]). In particular, for a bounded Lipschitz domain $\Omega \subset \mathbb{R}^3$, we refer to $L^2(\Omega)$ and $H^m(\Omega), m \in \mathbb{N}$, as the Hilbert space of Lebesgue integrable functions in Ω and the Sobolev space of functions with Lebesgue integrable generalized derivatives up to order m. Likewise, $\mathbf{L}^2(\Omega)$ and $\mathbf{H}^m(\Omega)$ stand for the corresponding Hilbert spaces of vector-valued functions. In both cases, the inner products and associated norms will be denoted by $(\cdot,\cdot)_{m,\Omega}$ and $\|\cdot\|_{m,\Omega}, m \geq 0$, respectively. For a function $v \in H^1(\Omega)$, we denote by $v|_\Gamma, \Gamma := \partial\Omega$, the trace of v on Γ and define $H_0^1(\Omega) := \{v \in H^1(\Omega) \mid v|_\Gamma = 0\}$. Moreover, we denote by $\mathbf{H}(\mathbf{curl};\Omega) := \{\mathbf{v} \in \mathbf{L}^2(\Omega) \mid \mathbf{curl}\ \mathbf{v} \in \mathbf{L}^2(\Omega)\}$ and $\mathbf{H}(\mathrm{div},\Omega) := \{\mathbf{v} \in \mathbf{L}^2(\Omega) \mid \mathrm{div}\ \mathbf{v} \in L^2(\Omega)\}$ the Hilbert spaces of vector-valued functions with the inner products $(\cdot,\cdot)_{\mathrm{curl},\Omega}, (\cdot,\cdot)_{\mathrm{div},\Omega}$ and associated norms $\|\cdot\|_{\mathrm{curl},\Omega}, \|\cdot\|_{\mathrm{div},\Omega}$. We refer to $\mathbf{H}_0(\mathbf{curl};\Omega) := \{\mathbf{v} \in \mathbf{H}(\mathbf{curl};\Omega) \mid \boldsymbol{\pi}_t(\mathbf{v}) = 0 \text{ on } \Gamma\}$ as the subspace of vector fields with vanishing tangential trace components $\boldsymbol{\pi}_t(\mathbf{v}) := \mathbf{n}_\Gamma \wedge (\mathbf{v} \wedge \mathbf{n}_\Gamma)$ on Γ, where $\mathbf{n}_\Gamma$ stands for the exterior unit normal vector on Γ. We further denote by $\boldsymbol{\gamma}_t(\mathbf{v}) := \mathbf{v} \wedge \mathbf{n}_\Gamma$ the tangential trace of $\mathbf{v}$ on Γ. We note that for $\mathbf{v} \in \mathbf{H}(\mathbf{curl};\Omega)$ there holds $\boldsymbol{\pi}_t(\mathbf{v}) \in \mathbf{H}^{-1/2}(\mathbf{curl}_\Gamma;\Gamma)$ and $\boldsymbol{\gamma}_t(\mathbf{v}) \in \mathbf{H}^{-1/2}(\mathrm{div}_\Gamma;\Gamma)$, where $\mathbf{curl}_\Gamma$ and div_Γ stand for the tangential **curl** and the tangential div (cf., e.g., [10]).

We consider the following control constrained $\mathbf{H}(\mathbf{curl})$-elliptic optimal control problem: Find $(\mathbf{y},\mathbf{u}) \in \mathbf{V} \times \mathbf{K}$ such that

$$\min_{(\mathbf{y},\mathbf{u})\in\mathbf{V}\times\mathbf{K}} J(\mathbf{y},\mathbf{u}) := \frac{1}{2}\,\|\mathbf{curl}\mathbf{y} - \mathbf{y}^d\|_{0,\Omega}^2 \;+\; \frac{\alpha}{2}\,\|\mathbf{u}-\mathbf{u}^d\|_{0,\Omega}^2 \tag{2.1a}$$

subject to the state equation

$$\mathbf{curl}\mu^{-1}\mathbf{curl}\mathbf{y} + \sigma\mathbf{y} = \mathbf{f} + \mathbf{u} \quad \text{in } \Omega, \tag{2.1b}$$

$$\boldsymbol{\pi}_t(\mathbf{y}) = \mathbf{g} \quad \text{on } \Gamma. \tag{2.1c}$$

Here, $\Omega \subset \mathbb{R}^3$ stands for a bounded Lipschitz polyhedral domain with boundary $\Gamma = \partial\Omega$, $\mathbf{y}^d \in \mathbf{H}_0(\mathbf{curl};\Omega), \mathbf{u}^d \in \mathbf{L}^2(\Omega), \alpha > 0$, $\mathbf{f} \in \mathbf{L}^2(\Omega)$, and $\mathbf{g} \in \mathbf{H}^{-1/2}(\mathbf{curl}_\Gamma;\Gamma)$. Moreover, $\mathbf{V} := \{\mathbf{y} \in \mathbf{H}(\mathbf{curl};\Omega) \mid \boldsymbol{\pi}_t(\mathbf{y}) = \mathbf{g}\}, \mathbf{V}_0 := \mathbf{H}_0(\mathbf{curl};\Omega)$, and $\mathbf{K} \subset \mathbf{L}^2(\Omega)$ denotes the closed, convex set

$$\mathbf{K} := \{\mathbf{u} \in \mathbf{L}^2(\Omega) \mid \mathbf{u}(\mathbf{x}) \geq \boldsymbol{\psi}(\mathbf{x}) \text{ a.e. in } \Omega\},$$

where $\boldsymbol{\psi} : \Omega \to \mathbb{R}^3$ is a given vector field with componentwise affine functions. The functions $\mu, \sigma \in L^\infty(\Omega)$ are supposed to be piecewise polynomial satisfying $\mu(\mathbf{x}) \geq \mu_0 > 0$ and $\sigma(\mathbf{x}) \geq \sigma_0 > 0$ a.e. in Ω. For the subsequent analysis, we assume vanishing tangential trace components, i.e., we set $\mathbf{g} = \mathbf{0}$ in (2.1c), and hence $\mathbf{V} = \mathbf{V}_0$.

Under the above assumptions, it is easy to show that (2.1a)-(2.1c) admits a unique solution $(\mathbf{y}^*,\mathbf{u}^*) \in \mathbf{V} \times \mathbf{K}$. The necessary and sufficient optimality conditions invoke an adjoint state $\mathbf{p}^* \in \mathbf{V}$ and a multiplier $\boldsymbol{\lambda}^* \in \mathbf{L}^2(\Omega)$ such that the quadruple $(\mathbf{y}^*,\mathbf{u}^*,\mathbf{p}^*,\boldsymbol{\lambda}^*)$ satisfies the optimality system

$$a(\mathbf{y}^*,\mathbf{q}) = \ell_1(\mathbf{q}), \quad \forall \mathbf{q} \in \mathbf{V}, \tag{2.2a}$$

$$a(\mathbf{p}^*,\mathbf{q}) = \ell_2(\mathbf{q}), \quad \forall \mathbf{q} \in \mathbf{V}, \tag{2.2b}$$

$$\mathbf{u}^* - \mathbf{u}^d = \alpha^{-1}(\mathbf{p}^* - \boldsymbol{\lambda}^*), \tag{2.2c}$$

$$\boldsymbol{\lambda}^* \in \partial I_{\mathbf{K}}(\mathbf{u}^*). \tag{2.2d}$$

Here, $a : \mathbf{V} \times \mathbf{V} \to \mathbb{R}$ refers to the bilinear form

$$a(\mathbf{y},\mathbf{q}) := (\mu^{-1}\mathbf{curl}\mathbf{y}, \mathbf{curl}\mathbf{q})_{0,\Omega} + (\sigma\mathbf{y},\mathbf{q})_{0,\Omega}, \quad \mathbf{y},\mathbf{q} \in \mathbf{V}, \tag{2.3}$$

and the functionals $\ell_i \in \mathbf{V}^*, i = 1,2$, are given according to

$$\ell_1(\mathbf{q}) := (\mathbf{f} + \mathbf{u}^*, \mathbf{q})_{0,\Omega}, \quad \mathbf{q} \in \mathbf{V}, \tag{2.4a}$$

$$\ell_2(\mathbf{q}) := (\mathbf{y}^d - \mathbf{curl}\mathbf{y}^*, \mathbf{curl}\mathbf{q})_{0,\Omega}, \quad \mathbf{q} \in \mathbf{V}. \tag{2.4b}$$

Furthermore, $\partial I_{\mathbf{K}} : \mathbf{L}^2(\Omega) \to 2^{\mathbf{L}^2(\Omega)}$ denotes the subdifferential of the indicator function $I_{\mathbf{K}}$ of the constraint set $\mathbf{K}$ (cf., e.g., [23]). We note that (2.2d) can be equivalently written as the variational inequality

$$(\boldsymbol{\lambda}^*, \mathbf{u}^* - \mathbf{v})_{0,\Omega} \;\geq\; 0, \quad \forall \mathbf{v} \in \mathbf{K},$$

and the complementarity problem

$$-\boldsymbol{\lambda}^* \in \mathbf{L}^2_+(\Omega)\ ,\ \mathbf{u}^* - \boldsymbol{\psi} \in \mathbf{L}^2_+(\Omega)\ ,\ (\boldsymbol{\lambda}^*, \mathbf{u}^* - \boldsymbol{\psi})_{0,\Omega} = 0, \tag{2.5}$$

where $\mathbf{L}^2_+(\Omega)$ refers to the nonnegative cone in $\mathbf{L}^2(\Omega)$.

REMARK 2.1.

(i) Our a posteriori error analysis can be straightforwardly transferred to the unconstrained case $\mathbf{K} = \mathbf{L}^2(\Omega)$ as well as to the bilateral control-constraint case

$$\mathbf{K} = \{\mathbf{u} \in \mathbf{L}^2(\Omega) \mid \boldsymbol{\psi}(\mathbf{x}) \leq \mathbf{u}(\mathbf{x}) \leq \boldsymbol{\phi}(\mathbf{x}) \text{ a.e. in } \Omega\},$$

where $\boldsymbol{\phi} : \Omega \to \mathbb{R}^3$ is a given vector field with componentwise affine functions satisfying $\boldsymbol{\psi}(\mathbf{x}) \leq \boldsymbol{\phi}(\mathbf{x})$ a.e. in Ω.

(ii) The state equation (2.1b)-(2.1c) is highly related to the eddy current model, in which case the magnetic induction is given by the rotation of the state, i.e., $\mathbf{B} = \mathbf{curly}$. Therefore, from the application point of view, it is more important to optimize the rotation field **curly** rather than the field $\mathbf{y}$ itself. This is the reason for choosing the tracking-type objective functional (2.1a) with respect to **curly**. In this context, the field $\mathbf{y}^d$ could represent a desired magnetic induction or a target arising from some measurement.

2.2. Edge element approximation. We assume $(h_n)_{n\in\mathbb{N}_0}$ to be a strictly decreasing null sequence of positive real numbers and $(\mathcal{T}_h(\Omega))_{h_n}$ a nested family of simplicial triangulations of Ω such that μ and σ are elementwise polynomial on $\mathcal{T}_{h_0}(\Omega)$. For an element $T \in \mathcal{T}_h(\Omega)$, we denote by h_T the diameter of T and set $h := \max\{h_T \mid T \in \mathcal{T}_h(\Omega)\}$. For $D \subset \bar{\Omega}$, we refer to $\mathcal{E}_h(D)$ and $\mathcal{F}_h(D)$ as the sets of edges and faces of $T \in \mathcal{T}_h(\Omega)$ in D. For $F \in \mathcal{F}_h(D)$, we denote by h_F the diameter of F and by $\omega_F := \bigcup\{T \in \mathcal{T}_h(\Omega) \mid F \subset \partial T\}$ as the patch consisting of the union of elements sharing F as a common face. In the sequel, for two mesh dependent quantities A and B we use the notation $A \lesssim B$, if there exists a constant $C > 0$ independent of h such that $A \leq CB$.

For the discrete approximation of (2.1a)-(2.1c), we use the edge elements of Nédélec's first family

$$\mathbf{Nd}_1(T) := \{\mathbf{q} : T \to \mathbb{R}^3 \mid \mathbf{q}(\mathbf{x}) = \mathbf{a} + \mathbf{b} \wedge \mathbf{x},\ \forall \mathbf{x} \in T\},$$

which give rise to the curl-conforming edge element space [33]

$$\mathbf{Nd}_{1,0}(\Omega; \mathcal{T}_h(\Omega)) := \{\mathbf{q}_h \in \mathbf{H}_0(\mathbf{curl}; \Omega) \mid \mathbf{q}_h|_T \in \mathbf{Nd}_1(T),\ \forall T \in \mathcal{T}_h(\Omega)\}. \tag{2.6}$$

Setting $\mathbf{V}_h := \mathbf{Nd}_{1,0}(\Omega; \mathcal{T}_h(\Omega))$ and

$$\mathbf{K}_h := \{\mathbf{u}_h \in \mathbf{V}_h \mid \mathbf{u}_h(\mathbf{x}) \geq \boldsymbol{\psi}(\mathbf{x}) \text{ a.e. in } \Omega\},$$

the edge element approximation of the distributed optimal control problem (2.1a)-(2.1c) reads as follows: Find $(\mathbf{y}_h, \mathbf{u}_h) \in \mathbf{V}_h \times \mathbf{K}_h$ such that

$$\min_{(\mathbf{y}_h, \mathbf{u}_h) \in \mathbf{V}_h \times \mathbf{K}_h} J(\mathbf{y}_h, \mathbf{u}_h) := \frac{1}{2} \|\mathbf{curly}_h - \mathbf{y}^d\|^2_{0,\Omega} + \frac{\alpha}{2} \|\mathbf{u}_h - \mathbf{u}_h^d\|^2_{0,\Omega} \tag{2.7a}$$

$$\text{subject to} \quad a(\mathbf{y}_h, \mathbf{q}_h) = (\mathbf{u}_h, \mathbf{q}_h)_{0,\Omega}, \quad \forall \mathbf{q}_h \in \mathbf{V}_h, \tag{2.7b}$$

where $\mathbf{u}_h^d \in \mathbf{V}_h$ is some approximation of $\mathbf{u}^d$. The existence and uniqueness of a solution $(\mathbf{y}_h^*, \mathbf{u}_h^*) \in \mathbf{V}_h \times \mathbf{V}_h$ can be deduced as in the continuous regime. The discrete optimality system gives rise to a discrete adjoint state $\mathbf{p}_h^* \in \mathbf{V}_h$ and a discrete

multiplier $\boldsymbol{\lambda}_h^* \in \mathbf{V}_h$ such that the quadruple $(\mathbf{y}_h^*, \mathbf{u}_h^*, \mathbf{p}_h^*, \boldsymbol{\lambda}_h^*)$ satisfies

$$a(\mathbf{y}_h^*, \mathbf{q}_h) = \ell_{1,h}(\mathbf{q}_h), \quad \forall \mathbf{q}_h \in \mathbf{V}_h, \tag{2.8a}$$
$$a(\mathbf{p}_h^*, \mathbf{q}_h) = \ell_{2,h}(\mathbf{q}_h), \quad \forall \mathbf{q}_h \in \mathbf{V}_h, \tag{2.8b}$$
$$\mathbf{u}_h^* - \mathbf{u}_h^d = \alpha^{-1}(\mathbf{p}_h^* - \boldsymbol{\lambda}_h^*), \tag{2.8c}$$
$$\boldsymbol{\lambda}_h^* \in \partial I_{\mathbf{K}_h}(\mathbf{u}_h^*). \tag{2.8d}$$

Here, the functionals $\ell_{i,h} : \mathbf{V}_h \to \mathbb{R}, 1 \le i \le 2$, are given by

$$\ell_{1,h}(\mathbf{q}_h) := (\mathbf{f} + \mathbf{u}_h^*, \mathbf{q}_h)_{0,\Omega}, \quad \mathbf{q}_h \in \mathbf{V}_h, \tag{2.9a}$$
$$\ell_{2,h}(\mathbf{q}_h) := (\mathbf{y}^d - \mathbf{curl}\mathbf{y}_h^*, \mathbf{curl}\mathbf{q}_h)_{0,\Omega}, \quad \mathbf{q}_h \in \mathbf{V}_h. \tag{2.9b}$$

Again, (2.8d) can be stated as the complementarity problem

$$\boldsymbol{\lambda}_h^* \le 0 \ , \ \boldsymbol{\psi} - \mathbf{u}_h^* \le 0 \ , \ (\boldsymbol{\lambda}_h^*, \mathbf{u}_h^* - \boldsymbol{\psi})_{0,\Omega} = 0. \tag{2.10}$$

2.3. The residual-type a posteriori error estimator. The residual-type a posteriori error estimator η_h consists of element residuals and face residuals associated with the state equation (2.2a) and the adjoint equation (2.2b) according to

$$\eta_h := \Big(\sum_{T \in \mathcal{T}_h(\Omega)} \eta_T^2 + \sum_{F \in \mathcal{F}_h(\Omega)} \eta_F^2 \Big)^{1/2}, \tag{2.11}$$
$$\eta_T^2 := \sum_{i=1}^{2} ((\eta_{y,T}^{(i)})^2 + (\eta_{p,T}^{(i)})^2), \quad \eta_F^2 := \sum_{i=1}^{2} ((\eta_{y,F}^{(i)})^2 + (\eta_{p,F}^{(i)})^2).$$

Here, $\eta_{y,T}^{(i)}$ and $\eta_{p,T}^{(i)}, 1 \le i \le 2$, are given by

$$\eta_{y,T}^{(1)} := h_T \|\mathbf{f} + \mathbf{u}_h^* - \mathbf{curl}\mu^{-1}\mathbf{curl}\mathbf{y}_h^* - \sigma\mathbf{y}_h^*\|_{0,T}, \tag{2.12a}$$
$$\eta_{y,T}^{(2)} := h_T \|\mathrm{div}(\sigma\mathbf{y}_h^*)\|_{0,T}, \tag{2.12b}$$
$$\eta_{p,T}^{(1)} := h_T \|\mathbf{curl}\mathbf{y}^d - \mathbf{curl}\mu^{-1}\mathbf{curl}\mathbf{p}_h^* - \sigma\mathbf{p}_h^*\|_{0,T}, \tag{2.12c}$$
$$\eta_{p,T}^{(2)} := h_T \|\mathrm{div}(\sigma\mathbf{p}_h^*)\|_{0,T}. \tag{2.12d}$$

The face residuals $\eta_{y,F}^{(i)}$ and $\eta_{p,F}^{(i)}, 1 \le i \le 2$, read as follows

$$\eta_{y,F}^{(1)} := h_F^{1/2} \|[\boldsymbol{\gamma}_t(\mu^{-1}\mathbf{curl}\mathbf{y}_h^*)]_F\|_{0,F}, \tag{2.13a}$$
$$\eta_{y,F}^{(2)} := h_F^{1/2} \|\mathbf{n}_F \cdot [(\mathbf{f} + \mathbf{u}_h^* - \sigma\mathbf{y}_h^*)]_F\|_{0,F}, \tag{2.13b}$$
$$\eta_{p,F}^{(1)} := h_F^{1/2} \|[\boldsymbol{\gamma}_t(\mu^{-1}\mathbf{curl}\mathbf{p}_h^* + \mathbf{curl}\mathbf{y}_h^*)]_F\|_{0,F}, \tag{2.13c}$$
$$\eta_{p,F}^{(2)} := h_F^{1/2} \|\mathbf{n}_F \cdot [(\sigma\mathbf{p}_h^*)]_F\|_{0,F}, \tag{2.13d}$$

where $[\boldsymbol{\gamma}_t(\mu^{-1}\mathbf{curl}\mathbf{q}_h)]_F$ and $[\mathbf{q}_h]_F, \mathbf{q}_h \in \mathbf{V}_h$, denote the jumps of $\boldsymbol{\gamma}_t(\mu^{-1}\mathbf{curl}\mathbf{q}_h)$ and $\mathbf{q}_h$ across $F = T_+ \cap T_-, T_\pm \in \mathcal{T}_h(\Omega)$.

We will show reliability of η_h and its efficiency up to data oscillations $osc_h(\mathbf{y}^d), osc_h(\mathbf{u}^d)$,

and $osc_h(\mathbf{f})$ as given by

$$osc_h(\mathbf{y}^d) := \Big(\sum_{T\in\mathcal{T}_h(\Omega)} osc_T^2(\mathbf{y}^d)\Big)^{1/2}, \tag{2.14a}$$

$$osc_T(\mathbf{y}^d) := h_T\|\mathbf{curl}(\mathbf{y}^d - \mathbf{y}_h^d)\|_{0,T},\ T\in\mathcal{T}_h(\Omega),$$

$$osc_h(\mathbf{u}^d) := \Big(\sum_{T\in\mathcal{T}_h(\Omega)} osc_T^2(\mathbf{u}^d)\Big)^{1/2}, \tag{2.14b}$$

$$osc_T(\mathbf{u}^d) := h_T\|\mathbf{u}^d - \mathbf{u}_h^d\|_{0,T},\ T\in\mathcal{T}_h(\Omega),$$

$$osc_h(\mathbf{f}) := \Big(\sum_{T\in\mathcal{T}_h(\Omega)} osc_T^2(\mathbf{f})\Big)^{1/2}, \tag{2.14c}$$

$$osc_T(\mathbf{f}) := h_T\|\mathbf{f} - \mathbf{f}_h\|_{0,T},\ T\in\mathcal{T}_h(\Omega), \tag{2.14d}$$

where $\mathbf{y}_h^d, \mathbf{u}_h^d \in \mathbf{V}_h$ are approximations of $\mathbf{y}^d$ and $\mathbf{u}^d$. Furthermore, $\mathbf{f}_h$ is an element-wise polynomial approximation of $\mathbf{f}$ satisfying $\operatorname{div}\mathbf{f}_h|_T = 0$ for all $T\in\mathcal{T}_h(\Omega)$.

2.4. Dörfler marking and refinement. In the step MARK of the adaptive cycle (1.1), elements of the simplicial triangulation $\mathcal{T}_h(\Omega)$ are marked for refinement according to the information provided by the a posteriori error estimator. With regard to convergence and quasi-optimality of AFEMs, the bulk criterion from [15], now also known as Dörfler marking, is a convenient choice. Here, we select a set $\mathcal{M}$ of elements such that for some $\theta\in(0,1)$ there holds

$$\sum_{T\in\mathcal{M}}\Big(\eta_T^2 + \frac{1}{2}\sum_{F\in\mathcal{F}_h(T)}\eta_F^2\Big) \geq \theta \sum_{T\in\mathcal{T}_h(\Omega)}\Big(\eta_T^2 + \frac{1}{2}\sum_{F\in\mathcal{F}_h(T)}\eta_F^2\Big). \tag{2.15}$$

Elements of the triangulation $\mathcal{T}_h(\Omega)$ that have been marked for refinement are subdivided by the newest vertex bisection.

3. Reliability of the error estimator. In this section, we prove reliability of the residual a posteriori error estimator η_h in the sense that it provides an upper bound for the global discretization error.

THEOREM 3.1. *Let* $(\mathbf{y}^*,\mathbf{u}^*,\mathbf{p}^*,\boldsymbol{\lambda}^*)$ *and* $(\mathbf{y}_h^*,\mathbf{u}_h^*,\mathbf{p}_h^*,\boldsymbol{\lambda}_h^*)$ *be the unique solutions of* (2.2a)-(2.2d) *and* (2.8a)-(2.8d)*, respectively. Further, let* η_h *and* $osc_h(\mathbf{u}^d)$ *be the residual error estimator and the data oscillation as given by* (2.11) *and* (2.14b)*. Then, there holds*

$$\|\mathbf{y}^* - \mathbf{y}_h^*\|_{curl,\Omega} + \|\mathbf{p}^* - \mathbf{p}_h^*\|_{curl,\Omega} + \|\mathbf{u}^* - \mathbf{u}_h^*\|_{0,\Omega} + \|\boldsymbol{\lambda}^* - \boldsymbol{\lambda}_h^*\|_{0,\Omega} \lesssim \eta_h + osc_h(\mathbf{u}^d). \tag{3.1}$$

The proof of (3.1) will be given by a series of lemmas. Here, our strategy to deal with the lack of Galerkin orthogonality is to introduce an intermediate state $\mathbf{y}(\mathbf{u}_h^*)\in\mathbf{V}$ and an intermediate adjoint state $\mathbf{p}(\mathbf{u}_h^*)\in\mathbf{V}$ as follows: Find $(\mathbf{y}(\mathbf{u}_h^*),\mathbf{p}(\mathbf{u}_h^*))\in\mathbf{V}\times\mathbf{V}$ such that

$$a(\mathbf{y}(\mathbf{u}_h^*),\mathbf{q}) = (\mathbf{u}_h^*,\mathbf{q})_{0,\Omega},\quad \forall\mathbf{q}\in\mathbf{V}, \tag{3.2a}$$

$$a(\mathbf{p}(\mathbf{u}_h^*),\mathbf{q}) = (\mathbf{y}^d - \mathbf{curly}(\mathbf{u}_h^*),\mathbf{curlq})_{0,\Omega},\quad \forall\mathbf{q}\in\mathbf{V}. \tag{3.2b}$$

Choosing $\mathbf{q} = \mathbf{p}(\mathbf{u}_h^*) - \mathbf{p}^*$ in (3.2a) and $\mathbf{q} = \mathbf{y}(\mathbf{u}_h^*) - \mathbf{y}^*$ in (3.2b) and then using (2.2a)-(2.2b), it follows that

$$(\mathbf{p}^* - \mathbf{p}(\mathbf{u}_h^*), \mathbf{u}^* - \mathbf{u}_h^*)_{0,\Omega} = -\|\mathbf{curl}(\mathbf{y}^* - \mathbf{y}(\mathbf{u}_h^*))\|_{0,\Omega}^2, \tag{3.3}$$

and hence

$$(\mathbf{p}^* - \mathbf{p}(\mathbf{u}_h^*), \mathbf{u}^* - \mathbf{u}_h^*)_{0,\Omega} \leq 0. \tag{3.4}$$

In order to establish the reliability of the a posteriori error estimator η_h, we split the discretization error $\mathbf{y}^* - \mathbf{y}_h^*$ and $\mathbf{p}^* - \mathbf{p}_h^*$ according to

$$\begin{aligned} \mathbf{y}^* - \mathbf{y}_h^* &= (\mathbf{y}^* - \mathbf{y}(\mathbf{u}_h^*)) + (\mathbf{y}(\mathbf{u}_h^*) - \mathbf{y}_h^*), \\ \mathbf{p}^* - \mathbf{p}_h^* &= (\mathbf{p}^* - \mathbf{p}(\mathbf{u}_h^*)) + (\mathbf{p}(\mathbf{u}_h^*) - \mathbf{p}_h^*), \end{aligned}$$

and estimate the terms on the right-hand sides separately.

LEMMA 3.2. *Let* $(\mathbf{y}^*, \mathbf{u}^*, \mathbf{p}^*, \boldsymbol{\lambda}^*)$ *and* $(\mathbf{y}_h^*, \mathbf{u}_h^*, \mathbf{p}_h^*, \boldsymbol{\lambda}_h^*)$ *be the unique solutions of* (2.2a)-(2.2d) *and* (2.8a)-(2.8d)*, respectively. Further, let* $\mathbf{y}(\mathbf{u}_h^*) \in \mathbf{V}$ *and* $\mathbf{p}(\mathbf{u}_h^*) \in \mathbf{V}$ *be the intermediate state and intermediate adjoint state as given by* (3.2a)-(3.2b)*. Then, there holds*

$$\|\mathbf{y}(\mathbf{u}_h^*) - \mathbf{y}^*\|_{curl,\Omega} \lesssim \|\mathbf{u}^* - \mathbf{u}_h^*\|_{0,\Omega}, \tag{3.5a}$$
$$\|\mathbf{p}(\mathbf{u}_h^*) - \mathbf{p}^*\|_{curl,\Omega} \lesssim \|\mathbf{y}^* - \mathbf{y}(\mathbf{u}_h^*)\|_{0,\Omega}. \tag{3.5b}$$

Proof. The results are immediate consequences of the $\mathbf{V}$-ellipticity and boundedness of $a(\cdot,\cdot)$. □

Our goal now is to estimate the terms $\|\mathbf{y}(\mathbf{u}_h^*) - \mathbf{y}_h^*\|_{curl,\Omega}$ and $\|\mathbf{p}(\mathbf{u}_h^*) - \mathbf{p}_h^*\|_{curl,\Omega}$, where the main key tool for the estimate is the Schöberl quasi-interpolation operator $\boldsymbol{\Pi}_h : \mathbf{V} \to \mathbf{V}_h$. In view of [35, Theorem 1], for every $\mathbf{v} \in \mathbf{V}$, we can decompose $\mathbf{v} - \boldsymbol{\Pi}_h\mathbf{v}$ into

$$\mathbf{v} - \boldsymbol{\Pi}_h\mathbf{v} = \nabla\varphi + \mathbf{z}, \tag{3.6}$$

where $\varphi \in H_0^1(\Omega)$ and $\mathbf{z} \in \mathbf{V}$ satisfy

$$h_T^{-1}\ \|\varphi\|_{0,T} + \|\nabla\varphi\|_{0,T} \lesssim \|\mathbf{v}\|_{0,\omega_T}, \tag{3.7a}$$
$$h_T^{-1}\ \|\mathbf{z}\|_{0,T} + \|\mathbf{curlz}\|_{0,T} \lesssim \|\mathbf{curlv}\|_{0,\omega_T}. \tag{3.7b}$$

Here, the element patches $\omega_T, T \in \mathcal{T}_h(\Omega)$, are given by

$$\omega_T := \cup\{T' \in \mathcal{T}_h \mid T' \cap \tilde{\omega}_T \neq \emptyset\}, \quad \tilde{\omega}_T := \cup\{T' \in \mathcal{T}_h \mid \mathcal{N}_h(T') \cap \mathcal{N}_h(T) \neq \emptyset\}.$$

LEMMA 3.3. *Let* $(\mathbf{y}_h^*, \mathbf{u}_h^*, \mathbf{p}_h^*, \boldsymbol{\lambda}_h^*)$ *be the unique solution of* (2.8a)-(2.8d)*, and let* $\mathbf{y}(\mathbf{u}_h^*) \in \mathbf{V}$ *and* $\mathbf{p}(\mathbf{u}_h^*) \in \mathbf{V}$ *be the intermediate state and intermediate adjoint state as given by* (3.2a)-(3.2b)*. Then, there holds*

$$\|\mathbf{y}(\mathbf{u}_h^*) - \mathbf{y}_h^*\|_{curl,\Omega} + \|\mathbf{p}(\mathbf{u}_h^*) - \mathbf{p}_h^*\|_{curl,\Omega} \lesssim \eta_h. \tag{3.8}$$

Proof. In view of (2.2a) and (3.2a), for $\tilde{\mathbf{e}}_y := \mathbf{y}(\mathbf{u}_h^*) - \mathbf{y}_h^*$, the Galerkin orthogonality

$$a(\tilde{\mathbf{e}}_y, \mathbf{q}_h) = 0, \quad \forall \mathbf{q}_h \in \mathbf{V}_h,$$

holds true, from which we deduce

$$\begin{aligned}\|\tilde{\mathbf{e}}_y\|_{curl,\Omega}^2 &\lesssim a(\tilde{\mathbf{e}}_y, \tilde{\mathbf{e}}_y - \boldsymbol{\Pi}_h\tilde{\mathbf{e}}_y)\\ &= a(\mathbf{y}(\mathbf{u}_h^*), \tilde{\mathbf{e}}_y - \boldsymbol{\Pi}_h\tilde{\mathbf{e}}_y) - a(\mathbf{y}_h^*, \tilde{\mathbf{e}}_y - \boldsymbol{\Pi}_h\tilde{\mathbf{e}}_y)\\ &= (\mathbf{u}_h^*, \tilde{\mathbf{e}}_y - \boldsymbol{\Pi}_h\tilde{\mathbf{e}}_y)_{0,\Omega} - a(\mathbf{y}_h^*, \tilde{\mathbf{e}}_y - \boldsymbol{\Pi}_h\tilde{\mathbf{e}}_y)\\ &= (\mathbf{f} + \mathbf{u}_h^* - \sigma\mathbf{y}_h^*, \tilde{\mathbf{e}}_y - \boldsymbol{\Pi}_h\tilde{\mathbf{e}}_y)_{0,\Omega} - (\mu^{-1}\mathbf{curly}_h^*, \mathbf{curl}(\tilde{\mathbf{e}}_y - \boldsymbol{\Pi}_h\tilde{\mathbf{e}}_y))_{0,\Omega},\end{aligned} \tag{3.9}$$

Using the decomposition (3.6) with $\mathbf{v} = \tilde{\mathbf{e}}_y$ in (3.9) along with (3.7a)-(3.7b) and the finite overlap of the element patches $\omega_T, T \in \mathcal{T}_h(\Omega)$, results in

$$\|\mathbf{y}(\mathbf{u}_h^*) - \mathbf{y}_h^*\|_{curl,\Omega}^2 \lesssim \sum_{T\in\mathcal{T}_h(\Omega)} \eta_{y,T}^2 + \sum_{F\in\mathcal{F}_h(\Omega)} \eta_{y,F}^2. \tag{3.10}$$

On the other hand, in view of (2.8b) and (3.2b), for $\tilde{\mathbf{e}}_p := \mathbf{p}(\mathbf{u}_h^*) - \mathbf{p}_h^*$ we obtain

$$\begin{aligned}&\|\tilde{\mathbf{e}}_p\|_{curl,\Omega}^2 \lesssim a(\tilde{\mathbf{e}}_p, \tilde{\mathbf{e}}_p) = a(\tilde{\mathbf{e}}_p, \boldsymbol{\Pi}_h\tilde{\mathbf{e}}_p) + a(\tilde{\mathbf{e}}_p, \tilde{\mathbf{e}}_p - \boldsymbol{\Pi}_h\tilde{\mathbf{e}}_p) \;=\\ &= (\mathbf{curl}(\mathbf{y}_h^* - \mathbf{y}(\mathbf{u}_h^*)), \mathbf{curl}\boldsymbol{\Pi}_h\tilde{\mathbf{e}}_p)_{0,\Omega} + (\mathbf{y}^d - \mathbf{curly}(\mathbf{u}_h^*), \mathbf{curl}(\tilde{\mathbf{e}}_p - \boldsymbol{\Pi}_h\tilde{\mathbf{e}}_p))_{0,\Omega}\\ &\quad - a(\mathbf{p}_h^*, \tilde{\mathbf{e}}_p - \boldsymbol{\Pi}_h\tilde{\mathbf{e}}_p)\\ &= (\mathbf{curl}(\mathbf{y}_h^* - \mathbf{y}(\mathbf{u}_h^*)), \mathbf{curl}(\boldsymbol{\Pi}_h\tilde{\mathbf{e}}_p - \tilde{\mathbf{e}}_p))_{0,\Omega} + (\mathbf{curl}(\mathbf{y}_h^* - \mathbf{y}(\mathbf{u}_h^*)), \mathbf{curl}\tilde{\mathbf{e}}_p)_{0,\Omega}\\ &\quad + (\mathbf{y}^d - \mathbf{curly}(\mathbf{u}_h^*), \mathbf{curl}(\tilde{\mathbf{e}}_p - \boldsymbol{\Pi}_h\tilde{\mathbf{e}}_p))_{0,\Omega} - \; a(\mathbf{p}_h^*, \tilde{\mathbf{e}}_p - \boldsymbol{\Pi}_h\tilde{\mathbf{e}}_p)\\ &= (\mathbf{curl}(\mathbf{y}_h^* - \mathbf{y}(\mathbf{u}_h^*)), \mathbf{curl}\tilde{\mathbf{e}}_p)_{0,\Omega} + (\mathbf{y}^d - \mathbf{curly}_h^*, \mathbf{curl}(\tilde{\mathbf{e}}_p - \boldsymbol{\Pi}_h\tilde{\mathbf{e}}_p))_{0,\Omega}\\ &\quad - \; a(\mathbf{p}_h^*, \tilde{\mathbf{e}}_p - \boldsymbol{\Pi}_h\tilde{\mathbf{e}}_p)\\ &= (\mathbf{curl}(\mathbf{y}_h^* - \mathbf{y}(\mathbf{u}_h^*)), \mathbf{curl}\tilde{\mathbf{e}}_p)_{0,\Omega} + (\mathbf{y}^d - \mu^{-1}\mathbf{curlp}_h^* - \mathbf{curly}_h^*, \mathbf{curl}(\tilde{\mathbf{e}}_p - \boldsymbol{\Pi}_h\tilde{\mathbf{e}}_p))_{0,\Omega}\\ &\quad - \; (\sigma\mathbf{p}_h^*, \tilde{\mathbf{e}}_p - \boldsymbol{\Pi}_h\tilde{\mathbf{e}}_p)_{0,\Omega}.\end{aligned} \tag{3.11}$$

Then, using again the decomposition (3.6) with $\mathbf{v} = \tilde{\mathbf{e}}_p$ in (3.11) along with (3.7a)-(3.7b) and the finite overlap of the element patches $\omega_T, T \in \mathcal{T}_h(\Omega)$, it follows that

$$\|\mathbf{p}(\mathbf{u}_h^*) - \mathbf{p}_h^*\|_{curl,\Omega}^2 \lesssim \|\mathbf{y}(\mathbf{u}_h^*) - \mathbf{y}_h^*\|_{curl,\Omega}^2 + \sum_{T\in\mathcal{T}_h(\Omega)} \eta_{p,T}^2 + \sum_{F\in\mathcal{F}_h(\Omega)} \eta_{p,F}^2. \tag{3.12}$$

Finally, combining (3.10) and (3.12) allows to conclude (3.8). ∎

LEMMA 3.4. *Let* $(\mathbf{y}^*, \mathbf{u}^*, \mathbf{p}^*, \boldsymbol{\lambda}^*)$ *and* $(\mathbf{y}_h^*, \mathbf{u}_h^*, \mathbf{p}_h^*, \boldsymbol{\lambda}_h^*)$ *be the unique solutions of* (2.2a)-(2.2d) *and* (2.8a)-(2.8d)*, respectively. Furthermore, let* η_h *as well as* $osc_h(\mathbf{u}^d)$ *be the residual-type a posteriori error estimator and data oscillation as given by* (2.11) *and* (2.14b)*. Then, there holds*

$$\|\mathbf{u}^* - \mathbf{u}_h^*\|_{0,\Omega} + \|\boldsymbol{\lambda}^* - \boldsymbol{\lambda}_h^*\|_{0,\Omega} \lesssim \eta_h + osc_h(\mathbf{u}^d). \tag{3.13}$$

Proof. Taking (2.2c) and (2.8c) into account, we find

$$\begin{aligned}\alpha\|\mathbf{u}^* - \mathbf{u}_h^*\|_{0,\Omega}^2 &= (\boldsymbol{\lambda}_h^* - \boldsymbol{\lambda}^*, \mathbf{u}^* - \mathbf{u}_h^*)_{0,\Omega}\\ &+ (\mathbf{p}^* - \mathbf{p}_h^*, \mathbf{u}^* - \mathbf{u}_h^*)_{0,\Omega} + \alpha(\mathbf{u}^d - \mathbf{u}_h^d, \mathbf{u}^* - \mathbf{u}_h^*)_{0,\Omega}.\end{aligned} \tag{3.14}$$

Using (2.5) and (2.10), for the first term on the right-hand side in (3.14) it follows that

$$(\boldsymbol{\lambda}_h^* - \boldsymbol{\lambda}^*, \mathbf{u}^* - \mathbf{u}_h^*)_{0,\Omega} = \underbrace{(\boldsymbol{\lambda}_h^*, \mathbf{u}^* - \boldsymbol{\psi})_{0,\Omega}}_{\leq 0} + \underbrace{(\boldsymbol{\lambda}_h^*, \boldsymbol{\psi} - \mathbf{u}_h^*)_{0,\Omega}}_{= 0} \tag{3.15}$$
$$- \underbrace{(\boldsymbol{\lambda}^*, \mathbf{u}^* - \boldsymbol{\psi})_{0,\Omega}}_{= 0} - \underbrace{(\boldsymbol{\lambda}^*, \boldsymbol{\psi} - \mathbf{u}_h^*)_{0,\Omega}}_{\geq 0} \leq 0.$$

For the second and third term on the right-hand side in (3.14), in view of (3.4) and (3.8), an application of Young's inequality yields

$$(\mathbf{p}^* - \mathbf{p}_h^*, \mathbf{u}^* - \mathbf{u}_h^*)_{0,\Omega} = \underbrace{(\mathbf{p}^* - \mathbf{p}(\mathbf{u}_h^*), \mathbf{u}^* - \mathbf{u}_h^*)_{0,\Omega}}_{\leq 0} + (\mathbf{p}(\mathbf{u}_h^*) - \mathbf{p}_h^*, \mathbf{u}^* - \mathbf{u}_h^*)_{0,\Omega}$$
$$\leq \frac{\alpha}{4}\|\mathbf{u}^* - \mathbf{u}_h^*\|_{0,\Omega}^2 + \frac{1}{\alpha}\|\mathbf{p}(\mathbf{u}_h^*) - \mathbf{p}_h^*\|_{0,\Omega}^2 \leq \frac{\alpha}{4}\|\mathbf{u}^* - \mathbf{u}_h^*\|_{0,\Omega}^2 + \frac{1}{\alpha}\eta_h^2, \tag{3.16a}$$
$$\alpha(\mathbf{u}^d - \mathbf{u}_h^d, \mathbf{u}^* - \mathbf{u}_h^*)_{0,\Omega} \leq \frac{\alpha}{4}\|\mathbf{u}^* - \mathbf{u}_h^*\|_{0,\Omega}^2 + \alpha\|\mathbf{u}^d - \mathbf{u}_h^d\|_{0,\Omega}^2. \tag{3.16b}$$

Using (3.15) and (3.16a),(3.16b) in (3.14) gives

$$\|\mathbf{u}^* - \mathbf{u}_h^*\|_{0,\Omega}^2 \leq \frac{2}{\alpha^2}\eta_h^2 + 2osc_h^2(\mathbf{u}^d). \tag{3.17}$$

On the other hand, observing (2.2c) and (2.8c) as well as (3.5a),(3.5b),(3.8), and (3.17), for $\boldsymbol{\lambda}^* - \boldsymbol{\lambda}_h^*$ we obtain

$$\|\boldsymbol{\lambda}^* - \boldsymbol{\lambda}_h^*\|_{0,\Omega}^2 \leq 3\|\mathbf{p}^* - \mathbf{p}_h^*\|_{0,\Omega}^2 + 3\alpha^2\|\mathbf{u}^* - \mathbf{u}_h^*\|_{0,\Omega}^2 + 3\alpha^2\|\mathbf{u}^d - \mathbf{u}_h^d\|_{0,\Omega}^2 \tag{3.18}$$
$$\leq 3\Big(\|\mathbf{u}^* - \mathbf{u}_h^*\|_{0,\Omega} + \|\mathbf{p}(\mathbf{u}_h^*) - \mathbf{p}_h^*\|_{0,\Omega}\Big)^2 + 3\alpha^2\|\mathbf{u}^* - \mathbf{u}_h^*\|_{0,\Omega}^2 + 3\alpha^2\|\mathbf{u}^d - \mathbf{u}_h^d\|_{0,\Omega}^2$$
$$\leq (6 + 3\alpha^2)\|\mathbf{u}^* - \mathbf{u}_h^*\|_{0,\Omega}^2 + 6\eta_h^2 + 3\alpha^2 osc_h^2(\mathbf{u}^d)$$
$$\leq \left(\frac{2(6+3\alpha^2)}{\alpha^2} + 6\right)\eta_h^2 + 3(4 + 3\alpha^2)osc_h^2(\mathbf{u}^d).$$

The assertion now follows from (3.17) and (3.18). □

4. Efficiency of the error estimator. We establish the efficiency of η_h by means of the local bubble functions

$$b_T := 256\prod_{i=1}^{4}\lambda_i^T, \quad b_F := 27\prod_{i=1}^{3}\lambda_{F_i}^T.$$

Here, $\lambda_i^T, 1 \leq i \leq 4$, are the barycentric coordinates of $T \in \mathcal{T}_h(\Omega)$ associated with the vertices of T, and $\lambda_{F_i}^T, 1 \leq i \leq 3$, are the barycentric coordinates associated with the vertices of $F \in \mathcal{F}_h(\Omega)$. The norm equivalences

$$\|b_T^{1/2}p_h\|_{0,T} \leq \|p_h\|_{0,T} \lesssim \|b_T^{1/2}p_h\|_{0,T},\ p_h \in P_k(T),\ k \in \mathbb{N}, \tag{4.1a}$$
$$\|b_F^{1/2}p_h\|_{0,F} \leq \|p_h\|_{0,F} \lesssim \|b_F^{1/2}p_h\|_{0,F},\ p_h \in P_k(F),\ k \in \mathbb{N}, \tag{4.1b}$$

can be easily verified by an affine invariance argument.

THEOREM 4.1. *Let* $(\mathbf{y}^*, \mathbf{u}^*, \mathbf{p}^*, \boldsymbol{\lambda}^*)$ *and* $(\mathbf{y}_h^*, \mathbf{u}_h^*, \mathbf{p}_h^*, \boldsymbol{\lambda}_h^*)$ *be the unique solutions of* (2.2a)-(2.2d) *and* (2.8a)-(2.8d)*, respectively. Furthermore, let* η_h *and* $osc_h(\mathbf{y}^d), osc_h(\mathbf{f})$ *be the residual-type a posteriori error estimator and data oscillations as given in* (2.11), (2.14a)*, and* (2.14c)*. Then, there holds*

$$\eta_h \lesssim \|\mathbf{y}^* - \mathbf{y}_h^*\|_{curl,\Omega} + \|\mathbf{p}^* - \mathbf{p}_h^*\|_{curl,\Omega} + \|\mathbf{u}^* - \mathbf{u}_h^*\|_{0,\Omega} + osc_h(\mathbf{y}^d) + osc_h(\mathbf{f}). \quad (4.2)$$

The proof of the theorem will be given by a series of lemmas where we show local efficiency in the sense that - up to data oscillations - the element and face residuals can be bounded from above by the elementwise or patchwise discretization error.

LEMMA 4.2. *Under the assumptions of Theorem 4.1, there holds*

$$\eta_{y,T}^{(1)} \lesssim \|\mathbf{y}^* - \mathbf{y}_h^*\|_{curl,T} + h_T\|\mathbf{u}^* - \mathbf{u}_h^*\|_{0,T} + osc_T(\mathbf{f}), \quad (4.3a)$$

$$\eta_{p,T}^{(1)} \lesssim \|\mathbf{y}^* - \mathbf{y}_h^*\|_{curl,T} + \|\mathbf{p}^* - \mathbf{p}_h^*\|_{curl,T} + osc_T(\mathbf{y}^d), \quad (4.3b)$$

for every $T \in \mathcal{T}_h(\Omega)$.

Proof. Obviously, for every $T \in \mathcal{T}_h(\Omega)$, we have

$$(\eta_{y,T}^{(1)})^2 \leq 2\Big(h_T^2\|\mathbf{f}_h + \mathbf{u}_h^* - \mathbf{curl}\mu^{-1}\mathbf{curly}_h^* - \sigma\mathbf{y}_h^*\|_{0,T}^2 + osc_h^2(\mathbf{f})\Big). \quad (4.4)$$

The function $\mathbf{z}_h := (\mathbf{f}_h + \mathbf{u}_h^* - \mathbf{curl}\mu^{-1}\mathbf{curly}_h^* - \sigma\mathbf{y}_h^*)b_T$ is an admissible test function in (2.2a), and hence, applying (4.1a) and Stokes' theorem results in

$$\begin{aligned}
&h_T^2\|\mathbf{f}_h + \mathbf{u}_h^* - \mathbf{curl}\mu^{-1}\mathbf{curly}_h^* - \sigma\mathbf{y}_h^*\|_{0,T}^2 \\
&\lesssim h_T^2(\mathbf{f}_h + \mathbf{u}_h^* - \mathbf{curl}\mu^{-1}\mathbf{curly}_h^* - \sigma\mathbf{y}_h^*, \mathbf{z}_h)_{0,T} \\
&= h_T^2\Big((\mathbf{f} + \mathbf{u}^*, \mathbf{z}_h)_{0,T} - a(\mathbf{y}_h^*, \mathbf{z}_h) + (\mathbf{u}_h^* - \mathbf{u}^*, \mathbf{z}_h)_{0,T} + (\mathbf{f}_h - \mathbf{f}, \mathbf{z}_h)_{0,T}\Big) \\
&= h_T^2\Big(a(\mathbf{y}^* - \mathbf{y}_h^*, \mathbf{z}_h) + (\mathbf{u}_h^* - \mathbf{u}^*, \mathbf{z}_h)_{0,T} + (\mathbf{f}_h - \mathbf{f}, \mathbf{z}_h)_{0,T}\Big) \\
&\leq h_T^2\Big(\|\mathbf{y}^* - \mathbf{y}_h^*\|_{curl,T}\|\mathbf{z}_h\|_{curl,T} + (\|\mathbf{u}^* - \mathbf{u}_h^*\|_{0,T} + \|\mathbf{f}_h - \mathbf{f}\|_{0,T})\|\mathbf{z}_h\|_{0,T}\Big).
\end{aligned}$$

Finally, using Young's inequality, the inverse inequality

$$\|\mathbf{z}_h\|_{curl,T} \lesssim h_T^{-1}\|\mathbf{z}_h\|_{0,T}, \quad (4.5)$$

and (4.1a) as well as (4.4) give (4.3a).

Likewise, choosing $\mathbf{z}_h := (\mathbf{curly}_h^d - \mathbf{curl}\mu^{-1}\mathbf{curlp}_h^* - \sigma\mathbf{p}_h^*)b_T$ in (2.2b), we find

$$\begin{aligned}
&(\eta_{p,T}^{(1)})^2 \leq 2h_T^2\Big(\|\mathbf{curly}_h^d - \mathbf{curl}\mu^{-1}\mathbf{curlp}_h^* - \sigma\mathbf{p}_h^*\|_{0,T} + \|\mathbf{curl}(\mathbf{y}^d - \mathbf{y}_h^d)\|_{0,T}\Big) \\
&\lesssim 2h_T^2\Big((\mathbf{curl}(\mathbf{y}_h^d - \mathbf{curly}_h^*) - \mathbf{curl}\mu^{-1}\mathbf{curlp}_h^* - \sigma\mathbf{p}_h^*, \mathbf{z}_h)_{0,T} + \|\mathbf{curl}(\mathbf{y}^d - \mathbf{y}_h^d)\|_{0,T}\Big).
\end{aligned}$$

For the first term on the right-hand side we find

$$\begin{aligned}
&h_T^2(\mathbf{curl}(\mathbf{y}_h^d - \mathbf{curly}_h^*) - \mathbf{curl}\mu^{-1}\mathbf{curlp}_h^* - \sigma\mathbf{p}_h^*, \mathbf{z}_h)_{0,T} \\
&= h_T^2(\mathbf{y}_h^d - \mathbf{curly}_h^*, \mathbf{curlz}_h)_{0,T} - a(\mathbf{p}_h^*, \mathbf{z}_h) \\
&= h_T^2\Big(a(\mathbf{p}^* - \mathbf{p}_h^*, \mathbf{z}_h) + (\mathbf{curl}(\mathbf{y}_h^d - \mathbf{y}^d), \mathbf{z}_h)_{0,T} + (\mathbf{curl}(\mathbf{y}_h^* - \mathbf{y}^*), \mathbf{curlz}_h)_{0,T}\Big) \\
&\lesssim h_T^2\Big(\|\mathbf{p}^* - \mathbf{p}_h^*\|_{curl,T}\|\mathbf{z}_h\|_{curl,T} + \|\mathbf{curl}(\mathbf{y}^d - \mathbf{y}_h^d)\|_{0,T}\|\mathbf{z}_h\|_{0,T} \\
&\qquad + \|\mathbf{curl}(\mathbf{y}^* - \mathbf{y}_h^*)\|_{0,T}\|\mathbf{curlz}_h\|_{0,T}\Big).
\end{aligned}$$

Using again Young's inequality, (4.1a), and (4.5) allows to deduce (4.3b). □

LEMMA 4.3. *Under the assumptions of Theorem 4.1, there holds*

$$\eta_{y,T}^{(2)} \lesssim \|\mathbf{y}^* - \mathbf{y}_h^*\|_{0,T} + \|\mathbf{u}^* - \mathbf{u}_h^*\|_{0,T} + osc_h(\mathbf{f}), \tag{4.6a}$$

$$\eta_{p,T}^{(2)} \lesssim \|\mathbf{p}^* - \mathbf{p}_h^*\|_{0,T}, \tag{4.6b}$$

for every $T \in \mathcal{T}_h(\Omega)$.

Proof. For the proof of (4.6a) we choose ∇z_h, where $z_h := \mathrm{div}(\sigma \mathbf{y}_h^*)|_T b_T$, as an admissible test function in (2.2a). Taking advantage of $\mathrm{div}(\mathbf{u}_h^*|_T) = 0$ and (4.1a), we find

$$\begin{aligned}(\eta_{y,T}^{(2)})^2 &\lesssim h_T^2(\mathrm{div}(\mathbf{u}_h^* - \sigma\mathbf{y}_h^*), z_h)_{0,T} = h_T^2(\mathbf{u}_h^* - \sigma\mathbf{y}_h^*, \nabla z_h)_{0,T}\\ &= h_T^2\Big((\mathbf{f}_h + \mathbf{u}_h^* - (\mathbf{f} + \mathbf{u}^*), \nabla z_h)_{0,T} + (\sigma(\mathbf{y}^* - \mathbf{y}_h^*), \nabla z_h)_{0,T} + (\mathbf{f} - \mathbf{f}_h, \nabla z_h)_{0,T}\Big)\\ &\lesssim h_T^2\Big(\|\mathbf{u} - \mathbf{u}_h^*\|_{0,T} + \|\mathbf{y}^* - \mathbf{y}_h^*\|_{0,T} + \|\mathbf{f} - \mathbf{f}_h\|_{0,T}\Big)\|\nabla z_h\|_{0,T}.\end{aligned}$$

Then, an application of Young's inequality, the inverse inequality

$$\|\nabla z_h\|_{0,T} \lesssim h_T^{-1}\|z_h\|_{0,T},$$

and (4.1a) results in (4.6a).
On the other hand ∇z_h, where $z_h := \mathrm{div}(\sigma \mathbf{p}_h^*)|_T b_T$, is an admissible test function in (2.2b) whence

$$\begin{aligned}(\eta_{p,T}^{(2)})^2 &\lesssim h_T^2(\mathrm{div}(\sigma\mathbf{p}_h^*), z_h)_{0,T} = h_T^2(\sigma\mathbf{p}_h^*, \nabla z_h)_{0,T}\\ &= h_T^2(\sigma(\mathbf{p}_h^* - \mathbf{p}^*), \nabla z_h)_{0,T} \lesssim h_T^2\|\mathbf{p}^* - \mathbf{p}_h^*\|_{0,T}\|\nabla z_h\|_{0,T},\end{aligned}$$

and we deduce (4.6b) by the same arguments as before. □

LEMMA 4.4. *Under the assumptions of Theorem 4.1, there holds*

$$\eta_{y,F}^{(1)} \lesssim \|\mathbf{y}^* - \mathbf{y}_h^*\|_{curl,T_+\cup T_-} + \|\mathbf{u}^* - \mathbf{u}_h^*\|_{0,T_+\cup T_-} + \eta_{y,T_+}^{(1)} + \eta_{y,T_-}^{(1)}, \tag{4.7a}$$

$$\eta_{p,F}^{(1)} \lesssim \|\mathbf{p}^* - \mathbf{p}_h^*\|_{0,T_+\cup T_-} + \eta_{p,T_+}^{(1)} + \eta_{p,T_-}^{(1)}, \tag{4.7b}$$

for every $F \in \mathcal{F}_h(\Omega), F = T_+ \cap T_-, T_\pm \in \mathcal{T}_h(\Omega)$.

Proof. We extend $[\boldsymbol{\gamma}_t(\mu^{-1}\mathbf{curly}_h^*)]_F$ to a polynomial function $[\boldsymbol{\gamma}_t(\mu^{-1}\mathbf{curly}_h^*)]_{T_\pm}$ on $T_\pm$ such that

$$\|[\boldsymbol{\gamma}_t(\mu^{-1}\mathbf{curly}_h^*)]_{T_\pm}\|_{0,T_\pm} \lesssim h_{T_\pm}\|[\boldsymbol{\gamma}_t(\mu^{-1}\mathbf{curly}_h^*)]_F\|_{0,F}. \tag{4.8}$$

Using (4.1b), Stokes' theorem, and the fact that the associated extension $\tilde{\mathbf{z}}_h$ of $\mathbf{z}_h := [\boldsymbol{\gamma}_t(\mu^{-1}\mathbf{curly}_h^*)]_F b_F$ is an admissible test function in (2.2a), we obtain

$$\begin{aligned}(\eta_{y,F}^{(1)})^2 &\lesssim h_F([\boldsymbol{\gamma}_t(\mu^{-1}\mathbf{curly}_h^*)]_F, \mathbf{z}_h)_{0,F} = h_F\Big((-\mathbf{curl}\mu^{-1}\mathbf{curly}_h^*, \tilde{\mathbf{z}}_h)_{0,T_+\cup T_-}\\ &+ (\mu^{-1}\mathbf{curly}_h^*, \mathbf{curl}\tilde{\mathbf{z}}_h)_{0,T_+\cup T_-}\Big) = h_F\Big((\mathbf{f} + \mathbf{u}_h^* - \mathbf{curl}\mu^{-1}\mathbf{curly}_h^* - \sigma\mathbf{y}_h^*, \tilde{\mathbf{z}}_h)_{0,T_+\cup T_-}\\ &+ (\mu^{-1}\mathbf{curl}(\mathbf{y}_h^* - \mathbf{y}^*), \mathbf{curl}\tilde{\mathbf{z}}_h)_{0,T_+\cup T_-} + (\sigma(\mathbf{y}_h^* - \mathbf{y}^*), \tilde{\mathbf{z}}_h)_{0,T_+\cup T_-}\\ &+ (\mathbf{u}^* - \mathbf{u}_h^*, \tilde{\mathbf{z}}_h)_{0,T_+\cup T_-}\Big) \lesssim \Big(h_F\|\mathbf{curl}(\mathbf{y}^* - \mathbf{y}_h^*)\|_{0,T_+\cup T_-}\|\mathbf{curl}\tilde{\mathbf{z}}_h\|_{0,T_+\cup T_-}\\ &+ h_F\|\mathbf{y}^* - \mathbf{y}_h^*\|_{0,T_+\cup T_-}\|\tilde{\mathbf{z}}_h\|_{0,T_+\cup T_-} + h_F\|\mathbf{u}^* - \mathbf{u}_h^*\|_{0,T_+\cup T_-}\|\tilde{\mathbf{z}}_h\|_{0,T_+\cup T_-}\\ &+ (\eta_{y,T_+} + \eta_{y,T_-})\|\tilde{\mathbf{z}}_h\|_{0,T_+\cup T_-}\Big).\end{aligned}$$

We deduce (4.7a) by Young's inequality, (4.1b), and (4.8). The proof of (4.7b) follows the same lines. ∎

LEMMA 4.5. *Under the assumptions of Theorem 4.1, there holds*

$$\eta_{y,F}^{(2)} \lesssim \|\mathbf{y}^* - \mathbf{y}_h^*\|_{0,T_+\cup T_-} + \|\mathbf{u}^* - \mathbf{u}_h^*\|_{0,T_+\cup T_-} + \eta_{y,T_+}^{(2)} + \eta_{y,T_-}^{(2)} + osc_h(\mathbf{f}), \tag{4.9a}$$

$$\eta_{p,F}^{(2)} \lesssim \|\mathbf{p}^* - \mathbf{p}_h^*\|_{0,T_+\cup T_-} + \eta_{p,T_+}^{(1)} + \eta_{p,T_-}^{(1)}, \tag{4.9b}$$

for every $F \in \mathcal{F}_h(\Omega), F = T_+ \cap T_-, T_\pm \in \mathcal{T}_h(\Omega)$.

Proof. For every $F \in \mathcal{F}_h(\Omega), F = T_+ \cap T_-, T_\pm \in \mathcal{T}_h(\Omega)$, we have

$$(\eta_{y,F}^{(2)})^2 \le 2h_F\Big(\|\mathbf{n}_F \cdot [\mathbf{f}_h + \mathbf{u}_h^* - \sigma\mathbf{y}_h^*]_F\|_{0,F}^2 + \|\mathbf{n}_F \cdot [\mathbf{f} - \mathbf{f}_h]_F\|_{0,F}^2\Big). \tag{4.10}$$

As in the proof of (4.7a), we extend $\mathbf{n}_F \cdot [\mathbf{f}_h + \mathbf{u}_h^* - \sigma\mathbf{y}_h^*]_F$ to a polynomial function $\mathbf{n}_F \cdot [\mathbf{f}_h + \mathbf{u}_h^* - \sigma\mathbf{y}_h^*]_{T_\pm}$ on $T_\pm$ such that

$$\|\mathbf{n}_F \cdot [\mathbf{f}_h + \mathbf{u}_h^* - \sigma\mathbf{y}_h^*]_{T_\pm}\|_{0,T_\pm} \lesssim h_{T_\pm}\|\mathbf{n}_F \cdot [\mathbf{f}_h + \mathbf{u}_h^* - \sigma\mathbf{y}_h^*]_F\|_{0,F} \tag{4.11}$$

and take advantage of the fact that $\nabla\tilde{z}_h$, where $\tilde{z}_h$ stands for the associated extension of $z_h := \mathbf{n}_F \cdot [\mathbf{f}_h + \mathbf{u}_h^* - \sigma\mathbf{y}_h^*]_F b_F$, is an admissible test function in (2.2a). Using (4.1b), Green's formula as well as $(\mathbf{f}_h, \nabla\tilde{z}_h)_{0,T_\pm} = 0$ due to $\mathrm{div}\mathbf{f}_h|_{T_\pm} = 0$ and $\mathrm{div}\mathbf{u}_h^*|_{T_\pm} = 0$, it follows that

$$\begin{aligned}
&h_F\|\mathbf{n}_F \cdot [\mathbf{f}_h + \mathbf{u}_h^* - \sigma\mathbf{y}_h*]_F\|_{0,F}^2 \\
&\lesssim h_F(\mathbf{n}_F \cdot (\mathbf{f}_h + \mathbf{u}_h^* - \sigma\mathbf{y}_h^*), z_h)_{0,F} = h_F\Big((\mathrm{div}(\sigma\mathbf{y}_h^*), \tilde{z}_h)_{0,T_+\cup T_-} \\
&+ \ (\mathbf{u}_h^* - \mathbf{u}^* - \sigma(\mathbf{y}_h^* - \mathbf{y}^*), \nabla\tilde{z}_h)_{0,T_+\cup T_-}\Big) \lesssim h_F\Big(\|\mathbf{y}^* - \mathbf{y}_h^*\|_{0,T_+\cup T_-}\|\nabla\tilde{z}_h\|_{0,T_+\cup T_-} \\
&+ \ \|\mathbf{u}^* - \mathbf{u}_h^*\|_{0,T_+\cup T_-}\|\nabla\tilde{z}_h\|_{0,T_+\cup T_-} + (\eta_{y,T_+}^{(2)} + \eta_{y,T_-}^{(2)})\|\tilde{z}_h\|_{0,T_+\cup T_-}\Big).
\end{aligned}$$

Young's inequality, (4.1b), and (4.10),(4.11) give rise to (4.9a). The proof of (4.9b) can be accomplished in a similar way. ∎

5. Numerics. We consider two examples for the optimal control problem (2.1) with exact solutions featuring jump discontinuities and nonempty active sets. In the first example, we use a convex domain, whereas a nonconvex L-shaped domain is considered in the second one. All the numerical results presented below were implemented by a Python script using the Dolphin Finite Element Library [30] and a projected gradient algorithm (see [38]) for solving the optimal control problem (2.1).

5.1. Convex domain. We consider a rather simple convex domain

$$\Omega = (-0.5, 0.5)^3.$$

However, the material parameters σ and μ^{-1} are chosen to be discontinuous as follows:

$$\sigma = \begin{cases} 100 & \text{in } \Omega_c, \\ 1 & \text{in } \Omega \setminus \Omega_c, \end{cases} \qquad \mu^{-1} = \begin{cases} 0.1 & \text{in } \Omega_c, \\ 1 & \text{in } \Omega \setminus \Omega_c, \end{cases}$$

with $\Omega_c := \{\mathbf{x} \in \mathbb{R}^3 \mid \mathbf{x}_1^2 + \mathbf{x}_2^2 + \mathbf{x}_3^2 < 0.4^2\}$. Furthermore, the data involved in (P) are given by

$$\begin{cases} \alpha = 1, \\ \mathbf{y}^d \equiv \boldsymbol{\psi} \equiv (0,0,0)^T, \\ \mathbf{u}^d(\mathbf{x}) = 100(\chi_{\Omega_c}(\mathbf{x}), 0, 0)^T, \\ \mathbf{f}(\mathbf{x}) = \sigma\nabla\phi(\mathbf{x}) - 100(\chi_{\Omega_c}(\mathbf{x}), 0, 0)^T, \end{cases}$$

where χ_{Ω_c} denotes the characteristic function of Ω_c, and the scalar function ϕ is defined by

$$\phi(\mathbf{x}) := \frac{1}{2\pi}\sin(2\pi\mathbf{x}_1)\sin(2\pi\mathbf{x}_2)\sin(2\pi\mathbf{x}_3).$$

Then, using the identity $\mathbf{curl}\nabla \equiv 0$, we infer that the unique solution for the optimal control problem (2.1) is given by

$$\mathbf{y}^* = \nabla\phi \quad \text{and} \quad \mathbf{u}^* = \mathbf{u}^d = 100(\chi_{\Omega_c}, 0, 0)^T.$$

We underline that the optimal control $\mathbf{u}^*$ features strong jump discontinuities across the interface $\partial\Omega_c$. Also, note that the lower bound $\boldsymbol{\psi}$ is *active* in $\Omega \setminus \Omega_c$ since

$$\mathbf{u}^*(\mathbf{x}) = \boldsymbol{\psi}(\mathbf{x}) \quad \text{in } \Omega \setminus \Omega_c.$$

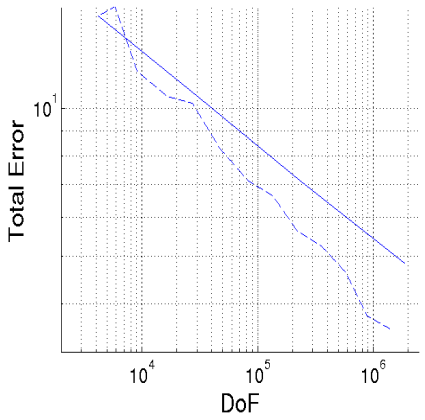

FIG. 5.1. *Total error for uniform (straight line) and adaptive mesh refinement (dash line).*

In Figure 5.1, we report on the computed total error

$$\|\mathbf{y}^* - \mathbf{y}_h^*\|_{curl,\Omega} + \|\mathbf{p}^* - \mathbf{p}_h^*\|_{curl,\Omega} + \|\mathbf{u}^* - \mathbf{u}_h^*\|_{0,\Omega}$$

resulting from the uniform mesh refinement compared with the one based on the adaptive mesh refinement using the proposed error estimator η_h. Here, DoF denotes the degrees of freedom in the finite element space $\mathbf{V}_h$. We conclude a better numerical performance of the adaptive method over the standard uniform mesh refinement. Note that the value $\theta = 0.8$ was used for the bulk criterion in the Dörfler marking. Furthermore, as plotted in Figure 5.2, the adaptive mesh refinement is concentrated around the interface $\partial\Omega_c$. This behavior is expected as the optimal control $\mathbf{u}^*$ is constructed to have jump discontinuities across the interface $\partial\Omega_c$. Table 5.1 presents the convergence history of the adaptive method and the computed effectivity index

$$\mathrm{I}_h = \frac{\eta_h}{\|\mathbf{y}^* - \mathbf{y}_h^*\|_{curl,\Omega} + \|\mathbf{p}^* - \mathbf{p}_h^*\|_{curl,\Omega} + \|\mathbf{u}^* - \mathbf{u}_h^*\|_{0,\Omega}}.$$

It is noticeable that the effectivity index I_h is close to 2.8.

TABLE 5.1
Convergence history and effectivity index.

DoF	$\|\mathbf{u}^* - \mathbf{u}_h^*\|_{0,\Omega}$	$\|\mathbf{y}^* - \mathbf{y}_h^*\|_{curl,\Omega}$	$\|\mathbf{p}^* - \mathbf{p}_h^*\|_{curl,\Omega}$	I_h
4184	13.342150	0.528396	1.547311	3.356047
5836	12.498939	0.613629	2.958597	3.051588
9072	10.587719	0.938416	0.352197	2.880237
16558	9.5027395	0.258851	0.829658	2.800450
27284	8.5995375	0.259084	1.360146	2.948251
47117	7.0834963	0.221773	0.978173	2.759841
83418	6.6135089	0.173759	0.334979	2.740255
135384	6.0651628	0.165448	0.400274	2.971874
218436	5.0086653	0.155864	0.486012	2.855683
362023	4.6907126	0.146354	0.392389	2.651461
577660	4.2936061	0.138599	0.194457	2.895985
884678	3.5363979	0.132519	0.122733	2.837530
1445806	3.3179560	0.113817	0.121641	2.708253

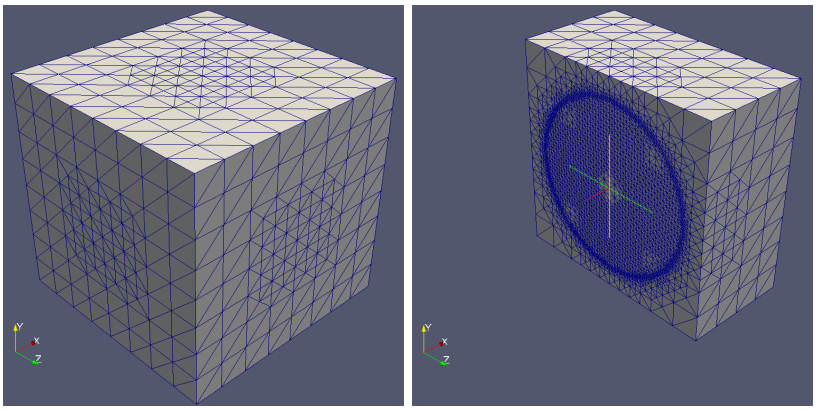

FIG. 5.2. *Adaptive mesh.*

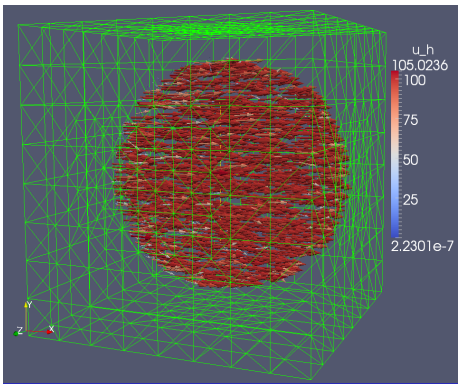

FIG. 5.3. *Computed optimal control on the finest adaptive mesh.*

5.2. Nonconvex L-shaped domain. We consider now a nonconvex L-shaped computational domain

$$\Omega = (-0.5, 0.5)^3 \setminus \{(0, 0.5) \times (-0.125, 0.5) \times (-0.5, 0.5)\}.$$

Similarly to the first example, the material parameters σ and μ^{-1} are chosen to be discontinuous

$$\sigma = \begin{cases} 100 & \text{in } \Omega_c := (-0.5, 0)^2 \times (0, 0.5), \\ 1 & \text{otherwise,} \end{cases} \qquad \mu^{-1} = \begin{cases} 0.1 & \text{in } \Omega_c, \\ 1 & \text{otherwise.} \end{cases}$$

All other data are set as in the previous example. Due to the nonconvex structure of the computational domain, the convergence of the uniform mesh refinement method, compared with the previous example, becomes slower. This slow convergence is somewhat expected from the analysis, since solutions of curl-curl problems on nonconvex polyhedral domains feature singularities at reentrant corners (see [14]). In this case, the performance of the adaptive method turns out to be more favorable in comparison with the previous example. Also, the adaptive method is able to capture the region where jump discontinuities and singularities are present in the solution (see Figure 5.5). The convergence history of the adaptive method is presented in Table 5.2. Here, the effectivity index is close to 3.

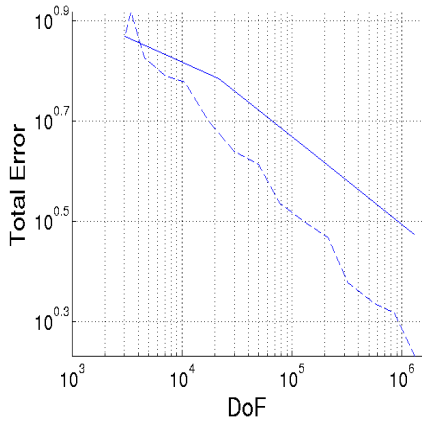

FIG. 5.4. *Total error for uniform (straight line) and adaptive mesh refinement (dash line).*

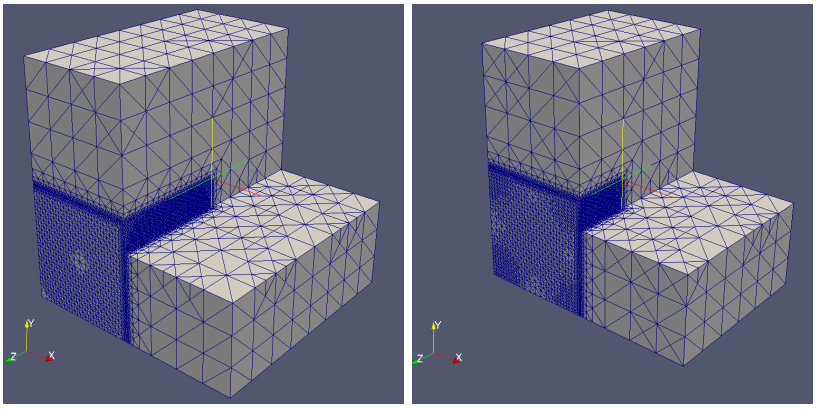

FIG. 5.5. *Adaptive mesh.*

TABLE 5.2
Convergence history and effectivity index.

DoF	$\|\mathbf{u}^* - \mathbf{u}_h^*\|_{0,\Omega}$	$\|\mathbf{y}^* - \mathbf{y}_h^*\|_{curl,\Omega}$	$\|\mathbf{p}^* - \mathbf{p}_h^*\|_{curl,\Omega}$	I_h
3004	6.199012	0.376819	0.820630	3.327702
3452	6.342518	0.400929	1.538389	3.171178
4583	5.547472	0.306768	0.842476	2.966337
7146	4.941834	0.286111	0.932936	2.871339
10584	4.844246	0.261587	0.872780	3.081036
17160	4.026743	0.241329	0.760033	2.920655
29926	3.635188	0.225424	0.500370	2.843312
49801	3.528143	0.217976	0.361220	3.008300
77056	2.887235	0.214939	0.325443	3.025875
135229	2.621580	0.213087	0.298890	2.843035
214402	2.534843	0.210963	0.179470	2.918438
321668	2.056567	0.204488	0.122065	2.938735
562580	1.872029	0.180525	0.109425	2.882065
853701	1.807420	0.165857	0.095384	3.018933
1300641	1.460198	0.157659	0.084676	2.941755

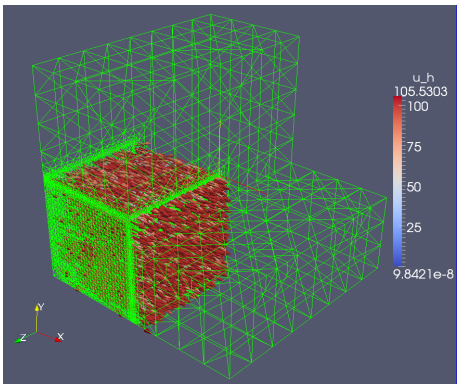

FIG. 5.6. *Computed optimal control on the finest adaptive mesh.*

REFERENCES

[1] M. Ainsworth and T. Oden, A Posteriori Error Estimation in Finite Element Analysis. Wiley, Chichester, 2000.
[2] H. Ammari, A. Buffa, and J.-C. Nédélec, A justification of eddy currents model for the Maxwell equations. SIAM J. Appl. Math. **60**, 1805–1823, 2000.
[3] D. Arnold, R. Falk, and R. Winther, Multigrid in H(div) and H(curl). Numer. Math. **85**, 197–217, 2000.
[4] D. Arnold, R. Falk, and R. Winther, Finite element exterior calculus, homological techniques, and applications. Acta Numerica **15** (2006), 1–155, 2006.
[5] I. Babuska and T. Strouboulis, The Finite Element Method and its Reliability. Clarendon Press, Oxford, 2001.
[6] W. Bangerth and R. Rannacher, Adaptive Finite Element Methods for Differential Equations. Lectures in Mathematics. ETH-Zürich. Birkhäuser, Basel, 2003.
[7] R. Beck, P. Deuflhard, R. Hiptmair, R.H.W. Hoppe, and B. Wohlmuth, Adaptive multilevel methods for edge element discretizations of Maxwell's equations. Surveys of Math. in Industry **8**, 271-312, 1999.
[8] R. Beck, R. Hiptmair, R.H.W. Hoppe, and B. Wohlmuth, Residual based a posteriori error estimators for eddy current computation. M^2AN Math. Modeling and Numer. Anal. **34**, 159-182, 2000.
[9] P. Binev, W. Dahmen, and R. DeVore, Adaptive finite element methods with convergence rates.

Numer. Math. **97**, 219-268, 2004.
[10] A. Buffa and P. Ciarlet, Jr., On traces for functional spaces related to Maxwell's equations. Part I: an integration by parts formula in Lipschitz polyhedra. Math. Meths. Appl. Sci. **24**, 9-30, 2001.
[11] C. Carstensen and R.H.W. Hoppe, Convergence analysis of an adaptive edge finite element method for the 2D eddy current equations. J. Numer. Math. **13**, 19-32, 2005.
[12] C. Carstensen and R.H.W. Hoppe, Unified framework for an a posteriori error analysis of non-standard finite element approximations of **H**(**curl**)-elliptic problems. J. Numer. Math. **17**, 27–44, 2009.
[13] J.M. Cascon, Ch. Kreuzer, R.H. Nochetto, and K.G. Siebert, Quasi-optimal rate of convergence of adaptive finite element methods. SIAM J. Numer. Anal. **46**, 2524–2550, 2008.
[14] M. Costabel and M. Dauge, Singularities of electromagnetic fields in polyhedral domains. Archive for Rational Mechanics and Analysis **151** 221–276, 2000.
[15] Dörfler, W.; A convergent adaptive algorithm for Poisson's equation. SIAM J. Numer. Anal. **33**, 1106–1124, 1996.
[16] K. Eriksson, D. Estep, P. Hansbo, and C. Johnson, Computational Differential Equations. Cambridge University Press, Cambridge, 1996.
[17] A. Gaevskaya, R.H.W. Hoppe, Y. Iliash, and M. Kieweg, Convergence analysis of an adaptive finite element method for distributed control problems with control constraints. In: Proc. Conf. Optimal Control for PDEs, Oberwolfach, Germany (G. Leugering et al.; eds.), Birkhäuser, Basel, 2007.
[18] M. Hintermüller and R.H.W. Hoppe, Goal-oriented adaptivity in control constrained optimal control of partial differential equations. SIAM J. Control Optim. **47**, 1721–1743, 2008.
[19] M. Hintermüller, R.H.W. Hoppe, Y. Iliash, and M. Kieweg, An a posteriori error analysis of adaptive finite element methods for distributed elliptic control problems with control constraints. ESAIM: Control, Optimisation and Calculus of Variations **14**, 540–560, 2008.
[20] M. Hinze, R. Pinnau, M. Ulbrich, S. Ulbrich, Optimization with PDE Constraints. Mathematical Modelling: Theory and Applications, Vol. 23, Springer, Berlin-Heidelberg-New York, 2008.
[21] R. Hiptmair, Multigrid method for Maxwell's equations. SIAM J. Numer. Anal. **36**, 204–225, 1999.
[22] R. Hiptmair, Finite elements in computational electromagnetism. Acta Numerica **11**, 237-339, 2002.
[23] J.B. Hiriart-Urruty and C. Lemaréchal, Convex Analysis and Minimization Algorithms. Springer, Berlin-Heidelberg-New York, 1993.
[24] R.H.W. Hoppe and J. Schöberl, Convergence of adaptive edge element methods for the 3D eddy currents equations. J. Comp. Math. **27**, 657–676, 2009.
[25] P. Houston, I. Perugia, and D. Schötzau, A posteriori error estimation for discontinuous Galerkin discretizations of $H(\mathrm{curl})$-elliptic partial differential equations. IMA Journal of Numerical Analysis **27**, 122–150, 2007.
[26] M. Kolmbauer and U. Langer A robust preconditioned Minres solver for distributed time-periodic eddy current optimal control problems. SIAM Journal on Scientific Computing, **34** B785–B809, 2012
[27] R. Li, W. Liu, H. Ma, and T. Tang, Adaptive finite element approximation for distributed elliptic optimal control problems. SIAM J. Control Optim. **41**, 1321–1349, 2002.
[28] X.J. Li and J. Yong, Optimal Control Theory for Infinite Dimensional Systems. Birkhäuser, Boston-Basel-Berlin, 1995.
[29] W. Liu and N. Yan, Adaptive Finite Element Methods for Optimal Control Governed by PDEs. Series in Information and Computational Science, Vol. 41. Global Science Press, Hong Kong, 2008.
[30] A. Logg, K.-A. Mardal, and G. N. Wells, Automated Solution of Differential Equations by the Finite Element Method. Springer, Boston, 2012.
[31] P. Monk, A posteriori error indicators for Maxwell's equations. J. Comp. Appl. Math. **100**, 173–190, 1998.
[32] P. Monk, Finite Element Methods for Maxwell Equations. Oxford University Press, Oxford, 2003.
[33] J.-C. Nédélec, Mixed finite elements in $\mathbb{R}^3$. Numer. Math. **35**, 315-341, 1980.
[34] P. Neittaanmäki and S. Repin, Reliable methods for mathematical modelling. Error control and a posteriori estimates. Elsevier, New York, 2004.
[35] J. Schöberl, A posteriori error estimates for Maxwell equations, Math. Comp. (2008) **77**, 633–649.
[36] R. Stevenson, Optimality of a standard adaptive finite element method. Found. Comput. Math.

7, 245-269, 2007.
[37] L. Tartar, Introduction to Sobolev Spaces and Interpolation Theory. Springer, Berlin-Heidelberg-New York, 2007.
[38] F. Tröltzsch, Optimal Control of Partial Differential Equations. Theory, Methods, and Applications. American Mathematical Society, Providence, 2010.
[39] F. Tröltzsch and I. Yousept, PDE–constrained optimization of time-dependent 3D electromagnetic induction heating by alternating voltages. ESAIM: M2AN **46**, 709–729, 2012.
[40] R. Verfürth, A Review of A Posteriori Estimation and Adaptive Mesh-Refinement Techniques. Wiley-Teubner, New York, Stuttgart, 1996.
[41] B. Vexler and W. Wollner, Adaptive finite elements for elliptic optimization problems with control constraints. SIAM J. Control Optim. **47**, 1150–1177, 2008.
[42] L. Zhong, L. Chen, S. Shu, G. Wittum, and J. Xu, Optimal error estimates of the Nedelec edge elements for time-harmonic Maxwell's equations, J. Comput. Math. **27** (2009), 563–572, 2009.
[43] I. Yousept, Optimal control of quasilinear $\boldsymbol{H}(\mathbf{curl})$-elliptic partial differential equations in magnetostatic field problems, SIAM J. Control and Optimization **51**, 3624–3651, 2013.
[44] I. Yousept, Optimal control of Maxwell's equations with regularized state constraints. Computational Optimization and Applications **52**, 59–581, 2012.
[45] I. Yousept, Finite element analysis of an optimal control problem in the coefficients of time-harmonic eddy current equations. Journal of Optimization Theory and Applications **154**, 879–903, 2012.
[46] L. Zhong, L. Chen, S. Shu, G. Wittum, and J. Xu, Convergence and optimality of adaptive edge finite element methods for time-harmonic Maxwell equations. Math. Comp. **81** , 623–642, 2012.